Acta Cryst E CRYSTALLOGRAPHIC COMMUNICATIONS

ISSN 2056-9890

Crystal structure and Hirshfeld surface analysis of 5-(3-nitro-1*H*-pyrazol-4-yl)-1*H*-tetrazole

Shannon E. Creegan,[a] James A. Ridenour,[b] Patrick A. Caruana,[a] Ian D. Giles[a] and Andrew T. Kerr[a]*

[a]US Naval Research Laboratory, Center for Biomolecular Science and Engineering, 4555 Overlook Ave., SW Washington, DC 20375, USA, and [b]US Naval Research Laboratory, Materials Chemistry and Dynamics Branch, 4555 Overlook Ave., SW Washington, DC 20375, USA. *Correspondence e-mail: andrew.t.kerr2.civ@us.navy.mil

Received 13 July 2025
Accepted 13 August 2025

Edited by M. Weil, Vienna University of Technology, Austria

Keywords: crystal structure; Huisgen reaction; pyrazole-substituted tetrazoles.

CCDC reference: 2480396

Supporting information: this article has supporting information at journals.iucr.org/e

5-(3-Nitro-1*H*-pyrazol-4-yl)tetrazole, $C_4H_3N_7O_2$, was synthesized from cyanopyrazole *via* the Huisgen reaction. The asymmetric unit contains two molecules, each displaying notable torsion between the pyrazole and tetrazole systems. N—H···N hydrogen bonds and π-stacking interactions create a double-wide molecular chain, while further N—H···N and weaker C—H···N interactions stitch these chains into a supramolecular hydrogen-bonded framework. From a Hirshfeld surface analysis, the closest contacts between molecules are through the N—H···N interactions between the tetrazole and pyrazole rings with N···H/H···N making up the largest contributing contacts in the fingerprint plot.

1. Chemical context

Heterocyclic systems are an area of interest due to their wide range of applications in energetic materials, pharmaceuticals, and dyes. These highly tailorable systems are useful for material characteristic modifications (*e.g.* solubility, polarity, density, *etc.*) and can be found in many natural products. As part of ongoing research, 5-(3-nitro-1*H*-pyrazol-4-yl)tetrazole was isolated following literature procedures (Shkineva *et al.*, 2022) utilizing the Huisgen reaction for the formation of pyrazole-substituted tetrazoles. This application of the Huisgen reaction occurs under standard conditions, refluxing 1,3-dipolar triethylammonium azide with a cyanopyrazole to synthesize a tetrazole.

2. Structural commentary

The title compound crystallizes in the orthorhombic Sohnke space group $P2_12_12_1$ with the asymmetric unit containing two molecules of 5-(3-nitro-1*H*-pyrazol-4-yl)tetrazole (Fig. 1; molecule 1: C1–C4, and molecule 2: C5–C8). All bond lengths are within expected range when compared to similar pyrazole/tetrazole systems (see section 5). The tetrazole and pyrazole rings are independently planar but non-planar to each other with N—C—C—C torsion angles of 40.8 (3)° in molecule 1 (N1—C1—C2—C4) and 41.9 (3)° in molecule 2 (N8—C5—C6—C8) (Fig. 2*a*). The non-planarity of each of the molecules is likely driven by steric hindrance from the nitro group, which is seen in other reported pyrazole-tetrazole molecules (Hanghong *et al.*, 2024; Kumbar *et al.*, 2018), and/or

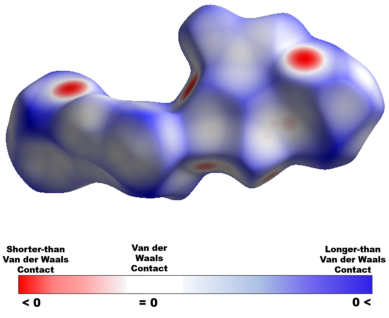

Table 1
Hydrogen-bond geometry (Å, °).

D—H···A	D—H	H···A	D···A	D—H···A
C7—H7···N3^{i}	0.93	2.51	3.420 (2)	167
N1—H1···N4^{ii}	0.86	2.06	2.840 (2)	151
N5—H5···N13^{iii}	0.86	2.14	2.968 (2)	162
N8—H8···N11^{ii}	0.86	2.02	2.830 (2)	157
N12—H12···N6	0.86	2.20	2.889 (2)	137
N12—H12···N10^{iv}	0.86	2.35	2.950 (2)	127

Symmetry codes: (i) $-x+\frac{1}{2}, -y+1, z+\frac{1}{2}$; (ii) $x+1, y, z$; (iii) $x-1, y, z$; (iv) $-x+1, y+\frac{1}{2}, -z+\frac{3}{2}$.

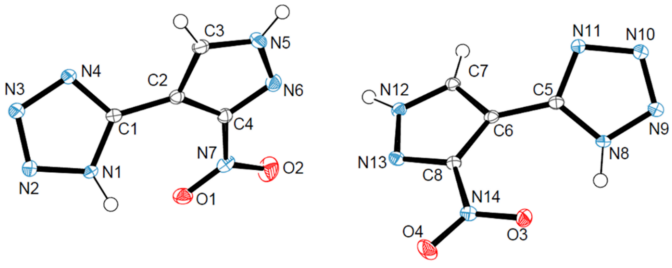

Figure 1
The two molecules [1 (C1 C4) and 2 (C5–C8)] in the asymmetric unit shown with displacement ellipsoids at the 50% probability level; H atoms are given as spheres of arbitrary radius.

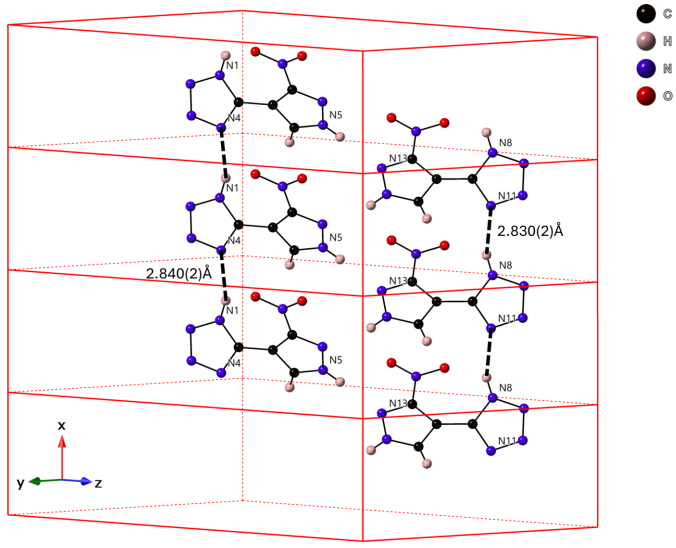

Figure 3
N—H···N hydrogen-bonding interactions (dotted lines) between symmetry-equivalent molecules (N1···N4 in molecule 1; N8···N11 in molecule 2) generating chains.

influenced by the dominant N—H···N supramolecular interactions discussed below.

3. Supramolecular features

The supramolecular packing interactions observed are primarily N—H···N and weaker C—H···N hydrogen-bonding interactions (Table 1). Each individual symmetrically equivalent molecule is hydrogen-bound together through N—H···N interactions, at N···N distances of 2.840 (2) Å for N1···N4 and 2.830 (2) Å for N8···N11, to make chains of molecule 1 and molecule 2 parallel to [100] (Fig. 3). Further, the tetrazole rings of molecules 1 and 2 are π-stacking at a $Cg\cdots Cg$ distance of 3.7936 (10) Å with a β angle of 19.5°, $Cg_{\rm perp}$ of 3.7178 (7) Å (Janiak, 2000), and a slippage of 1.269 Å to form a double-wide chain (Fig. 4). These chains further interact with one another to make a supramolecular frame-

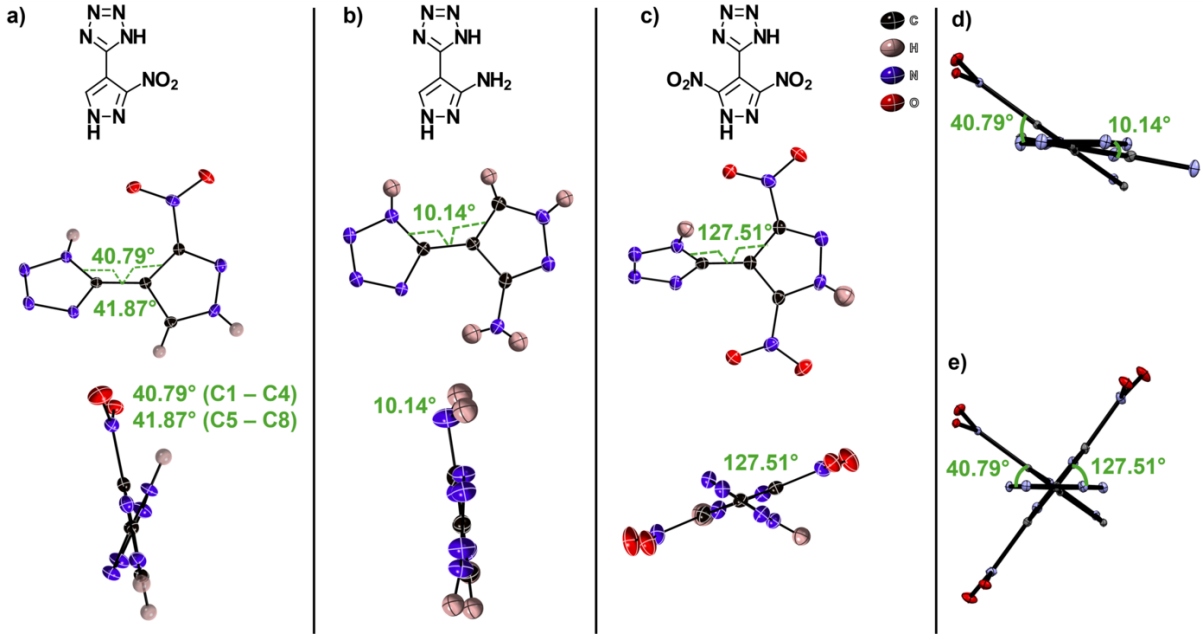

Figure 2
Molecular structures of (*a*) 5-(3-nitro-1*H*-pyrazol-4-yl)tetrazole and (*b*,*c*) of similar systems with torsion angles indicated; displacement ellipsoids are drawn at the 50% probability level. Structural overlay of the title compound with the amino (*d*) and dinitro (*e*) systems for comparison; displacement ellipsoids are drawn at the 10% probability level.

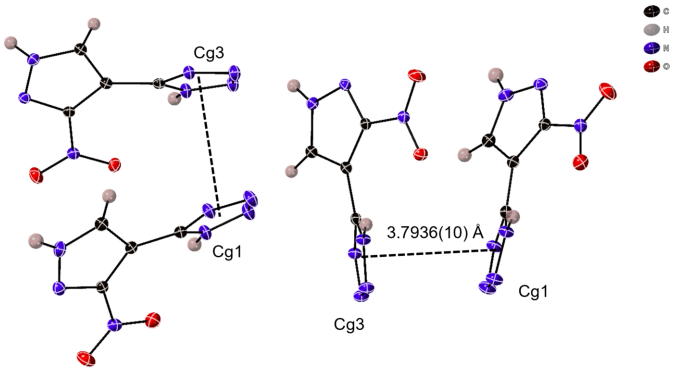

Figure 4
Molecules 1 and 2 are connected *via* π–π stacking interactions between *Cg*1 (containing N3) and *Cg*3 (containing N10).

work *via* a bifurcated N—H···N hydrogen bond [N12···N6 = 2.889 (2) Å, N12···N10 = 2.950 (2) Å], a single N—H···N interaction [N5···N13 = 2.968 (2) Å], and a C—H···N interaction [C7···N3 = 3.420 (2) Å], as shown in Fig. 5.

4. Hirshfeld surface analysis

The Hirshfeld surface (Fig. 6) and the associated two-dimensional fingerprint plots (Fig. 7) of the crystal structure were generated over d_{norm} using *CrystalExplorer* (Spackman *et al.*, 2021). The areas of closest contact are associated with N—H···N interactions between the tetrazole and pyrazole rings, seen as red areas in Fig. 6. From the fingerprint plots, N···H/H···N (31.5%) and N···O/O···N (18.4%) (Fig. 7*b*,*d*) contacts are the largest overall contributors, found in the lighter blue region of the fingerprint plot, with O···H/H···O (13.4%) (Fig. 7*c*) and N···N (10.9%) (Fig. 7*e*) contacts being midlevel contributors. Smaller contributions, less than 10%, are made by C···O/O···C (8.4%), N···C/C···N (6.7%), C···H/H···C (4.8%), O···O (3.4%) and H···H (2.3%) with the contribution of C···C contacts being less than 1%.

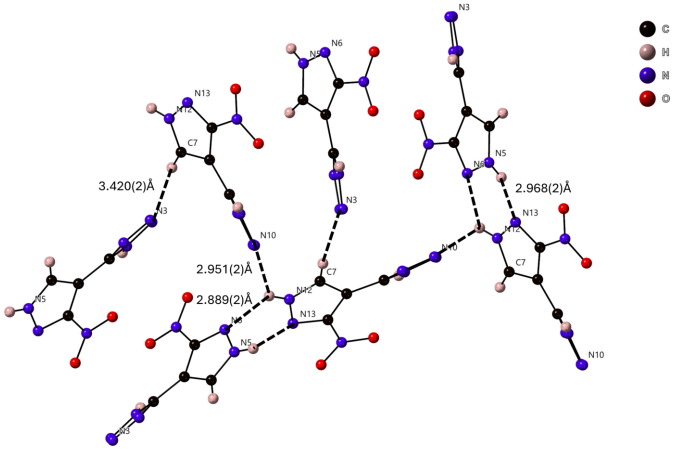

Figure 5
N—H···N hydrogen-bonding interactions between N5···N13, N12···N6 and N12···N10 as well as C—H···N interactions between C7···N3 weave the chains shown in Fig. 4 into a supramolecular framework.

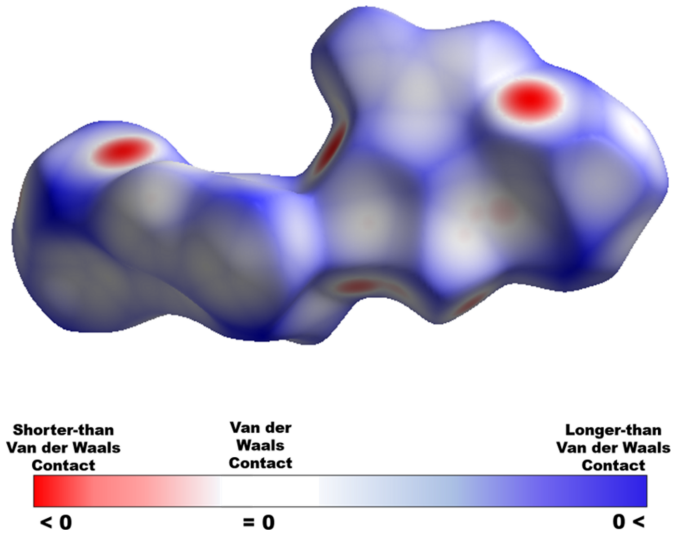

Figure 6
Hirshfeld surface displayed for the asymmetric unit. The region's color indicates if a contact distance is shorter than (red), equal to (white), or longer than (blue) the van der Waals separation.

5. Database survey

A search of the Cambridge Structural Database (CSD, version 5.46, update November 2024; Groom *et al.*, 2016) yielded twenty-four entries containing 5-(3-nitro-1*H*-pyrazol-4-yl) tetrazole as either a backbone structure or metal coordinating ligand. The most similar structures are 3-amino-4-tetrazole-pyrazole (ENAGAE; Deng *et al.*, 2019) and 3,5-dinitro-pyrazolyl-tetrazole (VUSRUZ; Benz *et al.*, 2020). The pyrazole and tetrazole rings exhibit the smallest torsion angle in the 3-amino structure, with a torsion angle of 10.14° (N1—C3—C1—C4) (Fig. 2*b*), while the dinitro group displays the most torsion, 126.51° (N8—C4—C2—C3) (Fig. 2*c*). The torsion angles are graphically compared to the title compound using *Mercury* (Macrae *et al.*, 2020) structure overlay plots in Fig. 2*d* and 2*e*.

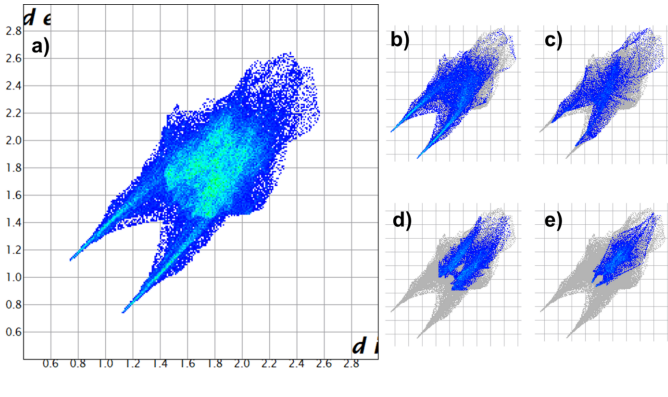

Figure 7
Fingerprint plots for the asymmetric unit of interactions greater than 10%; (*a*) all interactions, (*b*) N···H/H···N, (*c*) O···H/H···O, (*d*) N···O/O···N, (*e*) N···N interactions.

6. Synthesis and crystallization

5-(3-Nitro-1*H*-pyrazol-4-yl)tetrazole was synthesized according to a literature procedure (Shkineva *et al.*, 2022). A mixture of cyanopyrazole (0.497 g, 3.60 mmol), sodium azide (0.307 g, 4.72 mmol, 1.3 equiv.), triethylamine hydrochloride (0.6514 g, 4.73 mmol, 1.3 equiv.) and toluene (11 ml) was refluxed at 393 K for 16 h before cooling to ambient temperature. The resulting mixture was a clear, colorless liquid with yellow aggregates. Water (33 ml) was added to the mixture and stirred until all solids dissolved. The organic layer was removed and the aqueous layer acidified by the dropwise addition of hydrochloric acid until the pH was between 0 and 1. The solution turned a lighter shade of yellow without immediate precipitation and, after twenty minutes, the solution was extracted with ethyl acetate (3 × 50 ml). The solvent was dried over sodium sulfate and concentrated *in vacuo* resulting in a viscous yellow oil. Minimal ethyl acetate was added, and the mixture was chilled in an ice bath forming a precipitate that was isolated by filtration and washed with cold ethyl acetate (0.311 g; as a 94.5:5.5 mixture of product to starting material based by NMR, 45%). Slow evaporation of the filtrate yielded 0.147 g of additional material that contained a mixture of 20% product and 80% starting material. The single crystal used for analysis was obtained *via* slow evaporation from ethanol. ^{1}H NMR, (DMSO-d_6) δ: 14.59 (*br.s*, 1 H, NH); 8.64 (*s*, 1 H, CH).

7. Refinement

Crystal data, data collection, and structure refinement details are summarized in Table 2. All hydrogen atoms on carbon and nitrogen atoms were placed at their idealized positions and allowed to ride on the coordinates of their parent atoms [U_{iso}(H) fixed at 1.2U_{eq}(C,N)].

Table 2
Experimental details.

Crystal data	
Chemical formula	$C_4H_3N_7O_2$
M_r	181.13
Crystal system, space group	Orthorhombic, $P2_12_12_1$
Temperature (K)	100
a, b, c (Å)	4.9818 (1), 12.8064 (3), 21.5978 (5)
V (Å^3)	1377.92 (5)
Z	8
Radiation type	Cu $K\alpha$
μ (mm^{-1})	1.27
Crystal size (mm)	0.31 × 0.04 × 0.04
Data collection	
Diffractometer	Bruker Photon II CCD
Absorption correction	Multi-scan (*SADABS*; Krause *et al.*, 2015)
T_{min}, T_{max}	0.685, 0.754
No. of measured, independent and observed [$I > 2\sigma(I)$] reflections	14168, 2819, 2749
R_{int}	0.028
(sin $\theta/\lambda)_{max}$ (Å^{-1})	0.625
Refinement	
$R[F^2 > 2\sigma(F^2)]$, $wR(F^2)$, S	0.025, 0.061, 1.07
No. of reflections	2819
No. of parameters	235
H-atom treatment	H-atom parameters constrained
$\Delta\rho_{max}$, $\Delta\rho_{min}$ (e Å^{-3})	0.24, −0.22
Absolute structure	Flack x determined using 1109 quotients $[(I^+)-(I^-)]/[(I^+)+(I^-)]$ (Parsons *et al.*, 2013)
Absolute structure parameter	0.00 (6)

Computer programs: *APEX3* and *SAINT* (Bruker, 2019), *SHELXT* (Sheldrick, 2015*a*), *SHELXL* (Sheldrick, 2015*b*), *SHELXTL* (Sheldrick, 2008) and *publCIF* (Westrip, 2010).

Acknowledgements

We would like to thank the Office of Naval Research (ONR) and the U.S. Naval Research Laboratory (NRL) for their generous support of this base 6.1 program.

Funding information

Funding for this research was provided by: Office of Naval Research; U.S. Naval Research Laboratory.

References

Benz, M., Klapötke, T. M. & Stierstorfer, J. (2020). *Z. Anorg. Allg. Chem.* **646**, 1380–1388.

Bruker (2019). *APEX3* and *SAINT*. Bruker AXS Inc., Madison, Wisconsin, USA.

Deng, M., Feng, Y., Zhang, W., Qi, X. & Zhang, Q. (2019). *Nat. Commun.* **10**, 1339.

Groom, C. R., Bruno, I. J., Lightfoot, M. P. & Ward, S. C. (2016). *Acta Cryst.* B**72**, 171–179.

Hanghong, F., Jie, T., Caijin, L., Wei, H., Yang, H., Xiao, C. & Cheng, G. (2024). *Org. Lett.* **26**, 38, 8045–8050.

Janiak, C. (2000). *J. Chem. Soc. Dalton Trans.* pp. 3885–3896.

Krause, L., Herbst-Irmer, R., Sheldrick, G. M. & Stalke, D. (2015). *J. Appl. Cryst.* **48**, 3–10.

Kumbar, M. N., Kamble, R. R., Dasappa, J. P., Bayannavar, P. K., Khamees, H. A., Mahendra, M., Joshi, S. D., Dodamani, S., Rasal, V. P. & Jalalpure, S. (2018). *J. Mol. Struct.* **1160**, 63–72.

Macrae, C. F., Sovago, I., Cottrell, S. J., Galek, P. T. A., McCabe, P., Pidcock, E., Platings, M., Shields, G. P., Stevens, J. S., Towler, M. & Wood, P. A. (2020). *J. Appl. Cryst.* **53**, 226–235.

Parsons, S., Flack, H. D. & Wagner, T. (2013). *Acta Cryst.* B**69**, 249–259.

Sheldrick, G. M. (2008). *Acta Cryst.* A**64**, 112–122.

Sheldrick, G. M. (2015*a*). *Acta Cryst.* A**71**, 3–8.

Sheldrick, G. M. (2015*b*). *Acta Cryst.* C**71**, 3–8.

Shkineva, T. K., Serushkina, O. V., Vatsadze, I. A., Khoranyan, T. E. & Dalinger, I. L. (2022). *Russ. Chem. Bull.* **71**, 1737–1744.

Spackman, P. R., Turner, M. J., McKinnon, J. J., Wolff, S. K., Grimwood, D. J., Jayatilaka, D. & Spackman, M. A. (2021). *J. Appl. Cryst.* **54**, 1006–1011.

Westrip, S. P. (2010). *J. Appl. Cryst.* **43**, 920–925.

supporting information

Acta Cryst. (2025). E**81**, 861-864 [https://doi.org/10.1107/S2056989025007224]

Crystal structure and Hirshfeld surface analysis of 5-(3-nitro-1*H*-pyrazol-4-yl)-1*H*-tetrazole

Shannon E. Creegan, James A. Ridenour, Patrick A. Caruana, Ian D. Giles and Andrew T. Kerr

Computing details

5-(3-Nitro-1*H*-pyrazol-4-yl)-1*H*-tetrazole

Crystal data

$C_4H_3N_7O_2$
M_r = 181.13
Orthorhombic, $P2_12_12_1$
a = 4.9818 (1) Å
b = 12.8064 (3) Å
c = 21.5978 (5) Å
V = 1377.92 (5) Å^3
Z = 8
$F(000)$ = 736
D_x = 1.746 Mg m^{-3}
Cu $K\alpha$ radiation, λ = 1.54178 Å
Cell parameters from 9948 reflections
θ = 4.0–74.6°
μ = 1.27 mm^{-1}
T = 100 K
Rod, colorless
0.31 × 0.04 × 0.04 mm

Data collection

Bruker Photon II CCD diffractometer
Radiation source: 1uS microfocus
Montel multilayer optics monochromator
ω scans
Absorption correction: multi-scan (SADABS; Krause *et al.*, 2015)
T_{min} = 0.685, T_{max} = 0.754
14168 measured reflections
2819 independent reflections
2749 reflections with $I > 2\sigma(I)$
R_{int} = 0.028
θ_{max} = 74.5°, θ_{min} = 4.0°
h = −5→6
k = −14→16
l = −22→27

Refinement

Refinement on F^2
Least-squares matrix: full
$R[F^2 > 2\sigma(F^2)]$ = 0.025
$wR(F^2)$ = 0.061
S = 1.07
2819 reflections
235 parameters
0 restraints
Primary atom site location: dual
Hydrogen site location: inferred from neighbouring sites
H-atom parameters constrained
$w = 1/[\sigma^2(F_o^2) + (0.0325P)^2 + 0.3409P]$ where $P = (F_o^2 + 2F_c^2)/3$
$(\Delta/\sigma)_{max} < 0.001$
$\Delta\rho_{max}$ = 0.24 e Å^{-3}
$\Delta\rho_{min}$ = −0.22 e Å^{-3}
Absolute structure: Flack x determined using 1109 quotients $[(I^+)-(I^-)]/[(I^+)+(I^-)]$ (Parsons *et al.*, 2013)
Absolute structure parameter: 0.00 (6)

Special details

Experimental. The hydrogen peak determination was made following the experimental results published by Shkineva *et al.* of a broad singlet NH peak at 14.59 accounting for a single hydrogen and the pyrazole CH peak at 8.64 as a singlet inDMSO-d6. The lack of a second NH signal was not unexpected and can be mostly likely attributed to rapid exchange on the tetrazole ring. The tetrazole NH peak is usually a very broad singlet in the 15-16 ppm region and is difficult to separate from the baseline at lower concertation.

Geometry. All esds (except the esd in the dihedral angle between two l.s. planes) are estimated using the full covariance matrix. The cell esds are taken into account individually in the estimation of esds in distances, angles and torsion angles; correlations between esds in cell parameters are only used when they are defined by crystal symmetry. An approximate (isotropic) treatment of cell esds is used for estimating esds involving l.s. planes.

Fractional atomic coordinates and isotropic or equivalent isotropic displacement parameters (Å²)

	x	*y*	*z*	U_{iso}*/U_{eq}
C1	0.4100 (3)	0.62085 (13)	0.39918 (8)	0.0115 (3)
C2	0.3934 (3)	0.56191 (13)	0.45654 (8)	0.0118 (3)
C3	0.2011 (3)	0.48620 (13)	0.46685 (8)	0.0136 (3)
H3	0.073301	0.463185	0.438575	0.016*
C4	0.5297 (3)	0.56563 (14)	0.51357 (8)	0.0122 (3)
C5	0.7970 (3)	0.11907 (12)	0.72649 (7)	0.0104 (3)
C6	0.7960 (3)	0.20638 (13)	0.68310 (7)	0.0102 (3)
C7	0.6228 (3)	0.29043 (13)	0.68753 (8)	0.0109 (3)
H7	0.490779	0.300077	0.717445	0.013*
C8	0.9502 (3)	0.23144 (13)	0.63073 (8)	0.0105 (3)
N1	0.6270 (3)	0.65514 (11)	0.36902 (7)	0.0131 (3)
H1	0.790003	0.649609	0.381749	0.016*
N2	0.5496 (3)	0.69956 (13)	0.31571 (7)	0.0163 (3)
N3	0.2900 (3)	0.69265 (13)	0.31368 (7)	0.0172 (3)
N4	0.1961 (3)	0.64375 (12)	0.36525 (6)	0.0146 (3)
N5	0.2322 (3)	0.45188 (11)	0.52513 (7)	0.0158 (3)
H5	0.133196	0.404306	0.541515	0.019*
N6	0.4337 (3)	0.49950 (12)	0.55518 (7)	0.0151 (3)
N7	0.7521 (3)	0.63238 (12)	0.53093 (7)	0.0152 (3)
N8	1.0099 (3)	0.07153 (12)	0.75156 (7)	0.0123 (3)
H8	1.174939	0.083842	0.742439	0.015*
N9	0.9238 (3)	0.00135 (12)	0.79336 (7)	0.0145 (3)
N10	0.6635 (3)	0.00620 (12)	0.79306 (7)	0.0143 (3)
N11	0.5776 (3)	0.07882 (11)	0.75166 (6)	0.0121 (3)
N12	0.6802 (3)	0.35523 (11)	0.64088 (6)	0.0118 (3)
H12	0.596336	0.413000	0.634707	0.014*
N13	0.8801 (3)	0.32180 (11)	0.60472 (7)	0.0117 (3)
N14	1.1636 (3)	0.17244 (11)	0.60266 (7)	0.0124 (3)
O1	0.8497 (3)	0.68602 (10)	0.48967 (6)	0.0182 (3)
O2	0.8280 (3)	0.63091 (12)	0.58474 (6)	0.0276 (3)
O3	1.2290 (2)	0.09068 (9)	0.62874 (6)	0.0154 (3)
O4	1.2686 (3)	0.20548 (11)	0.55516 (6)	0.0230 (3)

Atomic displacement parameters (Å²)

	U^{11}	U^{22}	U^{33}	U^{12}	U^{13}	U^{23}
C1	0.0093 (7)	0.0124 (8)	0.0129 (8)	−0.0002 (6)	0.0002 (6)	−0.0010 (6)
C2	0.0099 (7)	0.0118 (8)	0.0137 (8)	0.0017 (6)	0.0005 (6)	−0.0005 (6)
C3	0.0100 (7)	0.0143 (8)	0.0164 (8)	−0.0001 (7)	−0.0004 (6)	0.0001 (7)
C4	0.0116 (7)	0.0121 (8)	0.0130 (8)	0.0019 (6)	0.0006 (6)	−0.0002 (6)
C5	0.0092 (7)	0.0110 (7)	0.0109 (7)	0.0000 (6)	0.0005 (6)	−0.0016 (6)
C6	0.0078 (6)	0.0125 (7)	0.0103 (7)	−0.0009 (6)	−0.0015 (6)	−0.0009 (6)
C7	0.0088 (7)	0.0131 (8)	0.0108 (8)	−0.0009 (6)	−0.0007 (6)	−0.0005 (6)
C8	0.0097 (7)	0.0111 (8)	0.0107 (8)	−0.0001 (6)	0.0002 (6)	−0.0009 (6)
N1	0.0077 (6)	0.0187 (7)	0.0131 (7)	0.0003 (5)	−0.0010 (5)	0.0033 (6)
N2	0.0123 (7)	0.0232 (8)	0.0134 (7)	0.0006 (6)	−0.0004 (6)	0.0054 (6)
N3	0.0117 (6)	0.0260 (8)	0.0139 (7)	−0.0002 (6)	−0.0006 (6)	0.0049 (6)
N4	0.0103 (6)	0.0212 (7)	0.0124 (7)	0.0000 (6)	−0.0004 (6)	0.0034 (6)
N5	0.0145 (7)	0.0145 (7)	0.0185 (7)	−0.0018 (6)	0.0026 (6)	0.0040 (6)
N6	0.0157 (7)	0.0152 (7)	0.0146 (7)	0.0030 (6)	0.0005 (5)	0.0014 (6)
N7	0.0125 (7)	0.0160 (7)	0.0170 (7)	0.0024 (6)	−0.0028 (6)	−0.0027 (6)
N8	0.0071 (6)	0.0155 (7)	0.0143 (7)	−0.0008 (5)	0.0008 (5)	0.0037 (6)
N9	0.0109 (7)	0.0163 (7)	0.0162 (7)	−0.0004 (6)	0.0012 (5)	0.0048 (6)
N10	0.0109 (7)	0.0162 (7)	0.0157 (7)	−0.0007 (6)	0.0004 (5)	0.0044 (6)
N11	0.0099 (6)	0.0138 (7)	0.0125 (7)	0.0002 (6)	0.0003 (5)	0.0024 (6)
N12	0.0103 (6)	0.0112 (6)	0.0138 (7)	0.0016 (5)	−0.0001 (5)	0.0000 (5)
N13	0.0116 (6)	0.0122 (7)	0.0113 (7)	−0.0004 (5)	0.0020 (5)	−0.0006 (6)
N14	0.0110 (7)	0.0130 (7)	0.0132 (7)	−0.0007 (5)	0.0012 (6)	−0.0008 (6)
O1	0.0135 (6)	0.0187 (6)	0.0225 (6)	−0.0032 (5)	−0.0002 (5)	0.0005 (5)
O2	0.0311 (8)	0.0337 (8)	0.0180 (7)	−0.0037 (7)	−0.0113 (6)	−0.0017 (6)
O3	0.0154 (6)	0.0140 (6)	0.0168 (6)	0.0044 (5)	0.0020 (5)	0.0027 (5)
O4	0.0250 (7)	0.0246 (7)	0.0195 (6)	0.0067 (6)	0.0142 (6)	0.0064 (5)

Geometric parameters (Å, º)

C1—N4	1.326 (2)	C8—N14	1.438 (2)
C1—N1	1.336 (2)	N1—N2	1.341 (2)
C1—C2	1.453 (2)	N1—H1	0.8600
C2—C3	1.381 (2)	N2—N3	1.297 (2)
C2—C4	1.407 (2)	N3—N4	1.361 (2)
C3—N5	1.342 (2)	N5—N6	1.342 (2)
C3—H3	0.9300	N5—H5	0.8600
C4—N6	1.324 (2)	N7—O2	1.222 (2)
C4—N7	1.449 (2)	N7—O1	1.226 (2)
C5—N11	1.325 (2)	N8—N9	1.344 (2)
C5—N8	1.337 (2)	N8—H8	0.8600
C5—C6	1.459 (2)	N9—N10	1.298 (2)
C6—C7	1.383 (2)	N10—N11	1.359 (2)
C6—C8	1.404 (2)	N12—N13	1.336 (2)
C7—N12	1.336 (2)	N12—H12	0.8600
C7—H7	0.9300	N14—O4	1.2269 (19)

C8—N13	1.333 (2)	N14—O3	1.2329 (19)
N4—C1—N1	107.95 (14)	C1—N1—H1	125.5
N4—C1—C2	122.69 (15)	N2—N1—H1	125.5
N1—C1—C2	129.23 (15)	N3—N2—N1	106.67 (14)
C3—C2—C4	102.55 (15)	N2—N3—N4	110.29 (14)
C3—C2—C1	122.81 (16)	C1—N4—N3	106.11 (14)
C4—C2—C1	134.51 (16)	N6—N5—C3	113.03 (14)
N5—C3—C2	107.52 (15)	N6—N5—H5	123.5
N5—C3—H3	126.2	C3—N5—H5	123.5
C2—C3—H3	126.2	C4—N6—N5	103.44 (14)
N6—C4—C2	113.46 (15)	O2—N7—O1	125.24 (16)
N6—C4—N7	118.54 (15)	O2—N7—C4	118.27 (15)
C2—C4—N7	127.99 (16)	O1—N7—C4	116.49 (14)
N11—C5—N8	108.11 (14)	C5—N8—N9	108.85 (13)
N11—C5—C6	123.96 (15)	C5—N8—H8	125.6
N8—C5—C6	127.73 (15)	N9—N8—H8	125.6
C7—C6—C8	102.66 (14)	N10—N9—N8	106.48 (14)
C7—C6—C5	123.67 (15)	N9—N10—N11	110.51 (15)
C8—C6—C5	133.67 (15)	C5—N11—N10	106.05 (14)
N12—C7—C6	107.31 (14)	N13—N12—C7	113.66 (14)
N12—C7—H7	126.3	N13—N12—H12	123.2
C6—C7—H7	126.3	C7—N12—H12	123.2
N13—C8—C6	113.23 (14)	C8—N13—N12	103.14 (13)
N13—C8—N14	118.17 (14)	O4—N14—O3	124.21 (14)
C6—C8—N14	128.59 (15)	O4—N14—C8	119.11 (14)
C1—N1—N2	108.98 (14)	O3—N14—C8	116.68 (14)
N4—C1—C2—C3	31.1 (3)	C2—C1—N4—N3	−176.02 (16)
N1—C1—C2—C3	−144.16 (19)	N2—N3—N4—C1	0.0 (2)
N4—C1—C2—C4	−144.0 (2)	C2—C3—N5—N6	0.0 (2)
N1—C1—C2—C4	40.8 (3)	C2—C4—N6—N5	0.00 (19)
C4—C2—C3—N5	−0.01 (18)	N7—C4—N6—N5	179.22 (14)
C1—C2—C3—N5	−176.40 (15)	C3—N5—N6—C4	0.00 (19)
C3—C2—C4—N6	0.0 (2)	N6—C4—N7—O2	−5.8 (2)
C1—C2—C4—N6	175.75 (18)	C2—C4—N7—O2	173.33 (17)
C3—C2—C4—N7	−179.12 (16)	N6—C4—N7—O1	174.02 (15)
C1—C2—C4—N7	−3.4 (3)	C2—C4—N7—O1	−6.9 (3)
N11—C5—C6—C7	37.2 (3)	N11—C5—N8—N9	−0.58 (18)
N8—C5—C6—C7	−137.05 (18)	C6—C5—N8—N9	174.39 (16)
N11—C5—C6—C8	−143.90 (18)	C5—N8—N9—N10	0.43 (19)
N8—C5—C6—C8	41.9 (3)	N8—N9—N10—N11	−0.1 (2)
C8—C6—C7—N12	0.15 (17)	N8—C5—N11—N10	0.50 (17)
C5—C6—C7—N12	179.35 (14)	C6—C5—N11—N10	−174.71 (15)
C7—C6—C8—N13	−0.28 (19)	N9—N10—N11—C5	−0.24 (19)
C5—C6—C8—N13	−179.36 (17)	C6—C7—N12—N13	0.02 (19)
C7—C6—C8—N14	−179.36 (16)	C6—C8—N13—N12	0.29 (18)
C5—C6—C8—N14	1.6 (3)	N14—C8—N13—N12	179.47 (14)

N4—C1—N1—N2	−0.21 (19)	C7—N12—N13—C8	−0.19 (18)
C2—C1—N1—N2	175.60 (17)	N13—C8—N14—O4	−1.9 (2)
C1—N1—N2—N3	0.2 (2)	C6—C8—N14—O4	177.14 (17)
N1—N2—N3—N4	−0.1 (2)	N13—C8—N14—O3	178.01 (14)
N1—C1—N4—N3	0.12 (19)	C6—C8—N14—O3	−3.0 (2)

Hydrogen-bond geometry (Å, º)

D—H···*A*	*D*—H	H···*A*	*D*···*A*	*D*—H···*A*
C7—H7···N3^{i}	0.93	2.51	3.420 (2)	167
N1—H1···N4^{ii}	0.86	2.06	2.840 (2)	151
N5—H5···N13^{iii}	0.86	2.14	2.968 (2)	162
N8—H8···N11^{ii}	0.86	2.02	2.830 (2)	157
N12—H12···N6	0.86	2.20	2.889 (2)	137
N12—H12···N10^{iv}	0.86	2.35	2.950 (2)	127

Symmetry codes: (i) −*x*+1/2, −*y*+1, *z*+1/2; (ii) *x*+1, *y*, *z*; (iii) *x*−1, *y*, *z*; (iv) −*x*+1, *y*+1/2, −*z*+3/2.